

Proceedings of the Korean Nuclear Society Autumn Meeting
Seoul, Korea, October 2001

Corrosion Kinetics of Ti-Al-Zr Alloy at 360°C in an Ammonia Water Chemistry

Tae-Kyu Kim, Jong-Hyuk Baek, Byung-Seon Choi, Yong-Hwan Jeong,

Doo-Jeong Lee, Moon-Hee Chang

Korea Atomic Energy Research Institute
P.O.Box 105, Yuseong, Daejeon 305-600, Korea

Abstract

The corrosion kinetics of Ti-Al-Zr alloy at 360 °C in a pH-9.98 ammonia water chemistry were evaluated. The alloy showed an excellent corrosion resistance, having a weight gain of 2.68 mg/dm² after 200 days. The hydrogen pick-up fraction during corrosion was revealed to be 23%. The oxide scale was mainly composed of anatase and rutile, and the corrosion rate decreased when rutile oxide was formed by the transformation from anatase oxide. The corrosion rate (K) with exposure time (t) was determined to be $\log K = -0.185 - 0.733 \log t$ (mg/dm²/day). The data calculated from the formula above have been verified to be in good agreement with the experimental results. Based on the corrosion rate and the hydrogen pickup fraction, it could be possible to predict the corrosion behavior and pick-up hydrogen content for prolonged periods when the transition in the corrosion rate was not considered.

1. Introduction

Ti-based alloys have drawn wide attention as candidate materials for heat-exchanging tubes in steam generators in a small-sized advanced integral PWR (Pressurized Water Reactor), due to its excellent corrosion resistance, good mechanical properties, attractive density, high neutron stability, and suitable durability characteristics [1-9]. Many studies have focused on improving the corrosion resistance of Ti-based alloys to work for prolonged periods [10-13]. Surface coating was shown to be an effective method to improve the oxidation resistance at elevated

temperatures [10-12]. The pre-oxidation of the Ti-4Al-2V alloy was also revealed to improve the corrosion resistance at 300°C in an alkaline steam. However, there is a shortage of the fundamental studies for the corrosion behavior of Ti-based alloys at high-temperatures and in high-pressure environments. This work studied the corrosion kinetics of Ti-Al-Zr alloy at 360 in an ammonia water chemistry. A corrosion process model was also proposed.

2. Experimental procedure

2.1 Sample

Ti-Al-Zr alloy tubes (10 mm OD × 7 mm ID) were prepared in extruded and mill-annealed conditions. The chemical composition is given in Table 1. A bright field transmission electron microscope (TEM) image in a parallel direction to the alloy tube revealed a fully recrystallization structure with an average grain size of about 20 μm (Fig. 1). Fig. 2 shows TEM/energy dispersive spectroscopy (EDS) studies on the precipitates in Ti-Al-Zr alloy. Two kinds of Fe-rich precipitates with the chemical formulations of TiFe and TiFe₂ were observed. Their sizes were examined to be in the 100-200 nm ranges. The precipitates of the TiFe phase with a chemical composition of (wt.%) 92.04Ti, 2.62Al, 4.36Zr, and 0.98Fe were usually found in the grains, but occasionally in the grain boundaries (Fig. 2a). The TiFe₂ precipitates with a chemical composition of (wt.%) 90.30Ti, 1.35Al, 4.60Zr, and 3.75Fe were occasionally detected in the grain boundaries (Fig. 2c).

2.2 Evaluation of corrosion behavior

The corrosion behavior was evaluated at 360 in a pH-9.98 alkaline solution containing 0.0001 mole NH₄OH under a pressure of 2,680 psi for 200 days using a circulating loop system. The water chemistries in the inlet of the heating zone (autoclave) were constantly maintained to be about a pH 9.98, 30 μg/L in DO (dissolved oxygen), 0.2 μg/L in DH (dissolved hydrogen), and 220 μS/L in conductivity, while those in the outlet were monitored to be about a pH 9.96, 60 μg/L in DO, 1.4 μg/L in DH, and 218 μS/L in conductivity. The corrosion rate was determined by using a gravimetric method. The hydrogen pick-up fraction was also evaluated.

3. Results and discussion

3.1 Corrosion kinetics

Fig. 3 shows the corrosion behavior of the Ti-Al-Zr alloy at 360 in a pH-9.98 ammonia

aqueous solution. It was apparent that the weight gain increased with increasing corrosion time. After exposure for 200 days, the weight gain was revealed to be 268 mg/dm² (Fig. 3a). With respect to the corrosion kinetics, it was observed that the corrosion rate was rapid in the initial period, but gradually decreased as the corrosion reaction proceeded (Fig. 3b).

The corrosion reaction of the Ti-based alloy with water to form titanium oxide appeared to be rapid in the early corrosion period, but the corrosion rate gradually decreased with an increase in the exposure time. These results imply that a layer of protective titanium oxide formed on the surface of the sample during corrosion would increase to disturb the diffusion of oxygen through the oxide layer, giving a decrease of corrosion rate as the corrosion reaction proceeded. Then, the corrosion rate (K) could be represented as following equation (1):

$$\log K = -0.185 - 0.733 \log \hat{\delta} \quad (1)$$

where K and $\hat{\delta}$ are the corrosion rate (in mg/dm².day) and exposure time (in days), respectively. The relationship of weight gain and exposure time could then be derived from equation (1), as follows:

$$WG_{\hat{\delta}} = K \times \hat{\delta} \quad (2)$$

where $WG_{\hat{\delta}}$, K, and $\hat{\delta}$ are the value of the weight gain (in mg/dm²), the corrosion rate (in mg/dm².day), and the exposure time (in days), respectively.

Fig. 4 shows the comparison of corrosion behavior obtained by experimental results with that calculated from equations (1) and (2) as a function of exposure time on the corrosion of the Ti-Al-Zr alloy. It can be seen that there is little difference between the experimental and calculated corrosion rates in the corrosion duration of 200 days (Fig. 4a); moreover, there is a good match between the experimental and calculated results on the weight gain (Fig. 4b). Thus, it could be concluded that equations (1) and (2) had a higher precision in the corrosion behavior of the alloy. Based on these results, it may be further possible to predict the corrosion behavior of the alloy after an exposure time of 200 days, if the transition in the corrosion rate is not considered.

3.2 XRD study the oxide scale

Fig. 5 shows the XRD patterns of the oxide scales formed on the surfaces of Ti-Al-Zr alloys corroded at 360 °C in a pH-9.98 ammonia aqueous solution for 30, 100 and 200 days. The several phases of titanium oxide, Ti₂O, TiO, α -Ti_{1-x}O and TiO₂ (anatase), were observed on the

oxide scale formed during oxidation for 30 days (Fig. 5a). As the corrosion reaction proceeded, the peak of anatase (TiO_2) on the sample corroded for 100 days was exhibited to be much higher than those found in the sample corroded for 30 days (Fig. 5b). Rutile (TiO_2) was also found in the oxide scale. As the corrosion reaction further proceeded, the peak of rutile was higher than that of anatase (Fig. 5c).

The oxide scale formed on the surface of the sample in the early period of corrosion was composed of several phases, Ti_2O , TiO , $\alpha\text{-Ti}_{1-x}\text{O}$ and anatase- TiO_2 (Fig. 5a). This indicates that the corrosion reaction of pure Ti follows these steps; $\text{Ti} \rightarrow \text{Ti}_2\text{O} \rightarrow \text{TiO} \rightarrow \alpha\text{-Ti}_{1-x}\text{O} \rightarrow \text{TiO}_2$. The peaks of pure Ti also appeared in the XRD patterns, since the depth of penetration of the X-ray was greater than the thickness of the oxide scale. As the corrosion reaction proceeded, the peak of anatase (TiO_2) on the sample corroded for 100 days appeared to be much higher than those found in the sample corroded for 30 days (Fig. 5b). The rutile (TiO_2) was also found in the oxide scale. Even the intermediate phases in the corrosion stages of pure Ti to TiO_2 , such as Ti_2O , TiO and $\alpha\text{-Ti}_{1-x}\text{O}$, would exist; it was hardly observed possibly due to their quantities being much less than the detection limit of the X-ray diffractometer. After 200 days, the peak of rutile was higher than that of anatase (Fig. 5c). The anatase is a metastable phase to be formed at a pressure below about 200,000 psi (13,788 bar) at 360 °C, while the rutile is a stable phase at all temperatures and ambient pressure [9]. This means that the transformation of anatase to rutile is possible and doesn't occur reversibly. From these results, these predictions would be possible; the oxide layer formed at the early stage was mainly composed of the anatase (Fig. 5b). As the corrosion reaction proceeded, the anatase previously formed would be transformed to the rutile (Fig. 5c). That is, the outer layer of the anatase oxide would be mainly composed of the rutile, while most of the inner layer of the oxide might be the anatase.

3.3 Hydrogen pick-up

Fig. 6 shows the hydrogen content and hydrogen pick-up fraction of the Ti-Al-Zr alloy with exposure time. It was observed that the hydrogen content slightly increased with exposure time, but the hydrogen pick-up rate maintained at an almost constant level of about 23%, showing itself to be almost independent of the exposure time. When Ti-based alloys are exposed to the primary coolant water in high-temperature and high-pressure environments, some of the hydrogen resulting from the reaction of Ti-alloys with water to form TiO_2 was picked up in the metal [3]. This means that the hydrogen content absorbed would be correlated with the corrosion rate, since the acceleration of the corrosion rate would produce more hydrogen content resulting from the oxidation reaction of titanium alloy with water. Thus, the pick-up

hydrogen content would be intimately correlated with the corrosion behavior. That is, the better resistance to the corrosion would provide the lower content of hydrogen absorbed into the metal. On the other hand, the hydrogen pick-up fraction was determined to be in the 23% range. This means that the 23% of the total hydrogen content produced by the corrosion reaction at the interface of metal-oxide would be picked up through the oxide layer, and absorbed into the metal. It is considered that this value is a relatively high level, since the titanium has a high affinity with hydrogen.

Fig. 7 shows the correlation of hydrogen pickup and oxygen weight gain in the corrosion of the Ti-Al-Zr alloy. It is well known that the corrosion reaction of the metal with oxygen produces hydrogen ions. The quantity of hydrogen ions produced is directly correlated with the corrosion rate, which is observed as the oxygen weight gain. In addition, the amount of picked up hydrogen could be expressed as hydrogen weight gain, since it also affects the weight gain. This means that there is a relationship between the hydrogen- and oxygen weight gains. When 100% of hydrogen produced by the corrosion reaction is picked up into the metal, it follows the solid line as shown in Fig. 7. The hydrogen pickup fraction in the present study is examined to be 23%, shown by the dotted line in Fig. 7.

3.4 Prediction of corrosion behavior and hydrogen content

Fig. 8 shows the expected corrosion behavior and hydrogen content of the Ti-Al-Zr alloy at 360 °C in a pH-9.98 ammonia aqueous solution. When it is considered that the transition in the corrosion rate does not occur, it would be possible to predict the corrosion behavior of the alloy for prolonged periods from equation (1). It is expected that the weight gain would continually increase, but the corrosion rate gradually decrease. On the other hand, the hydrogen pickup is intimately correlated with the weight gain. The pickup hydrogen content could be predicted based on a hydrogen pickup fraction of 23% (Fig. 6), since the hydrogen pickup fraction would maintain a constant value. It is expected that the hydrogen contents after 1000 and 2000 days would be 42.4 and 42.8 ppm, respectively.

3.5 Corrosion mechanism

Fig. 9 shows the corrosion mechanism of the Ti-Al-Zr alloy at 360 °C in a pH-9.98 ammonia aqueous solution. First, the oxygen and hydrogen ions from the water diffuse through the oxide layer to the metal. As a result of the corrosion reaction at the metal-oxide interface, the electrons would be produced. Then, the hydrogen ion would diffuse through the oxide layer to react with the electron to pick up into the metal. In the present study, 23% of the hydrogen ion

would pick up into the metal. At the same time, the excess electrons resulting from the corrosion reaction would diffuse through the oxide layer to the solution/oxide interface.

With respect to the oxide layer, the inner layer near the metal would be mainly composed of anatase oxide, while the outer layer would be near the solution rutile one (Fig. 5). In the solution, the corrosion reaction provided the increase in the DO and DH (from 30 and 0.2 ppb in inlet to 60 and 1.4 ppb in outlet), and slight decrease in the pH and conductivity (from pH 9.98 and 220 $\mu\text{S/L}$ in inlet to pH 9.96 and 218 $\mu\text{S/L}$ in outlet).

4. Summary

In this study, the corrosion behavior of the Ti-Al-Zr alloy for steam generator heat-exchanging tubes at 360 in a pH 9.98 alkaline solution containing NH_4OH were evaluated. The formula of corrosion rate (K) was determined to be $\log K = -0.185 - 0.733 \lg \delta$. In the experimental period of 200 days, the values of the weight gain calculated by the equation showed good agreement with the experimental results. The hydrogen pickup fraction was revealed to be 23%. Based on these results, the corrosion behavior and hydrogen content of this alloy for prolonged periods were predicted. The corrosion mechanism connected with the water chemistry was also proposed.

Acknowledgements

The authors would like to express their appreciation to the Ministry of Science and Technology (MOST) of the Republic of Korea for the support of this work through the mid- and long-term nuclear R&D project.

References

1. O.A. Kozhevnikow, E.V. Nesterova, V.V. Rybin and I.I. Yarmolovich: J. Nuclear Mater. 271&272 (1999) 472-477
2. Gorynin, I.V.: Materials Science and Engineering, A263 (1999) 112-116
3. M.L. Wasz, F.R. Brotzen, R.B. McLellan, and A.J. Griffin, Jr: International Materials Reviews 41 (1) (1996) pp. 1-12
4. J.C. Williams: M Materials Science and Engineering, A263 (1999) 107-111
5. D.G. Kolman and J.R. Scully: J. Electrochem. Soc. 143 (1996) 1847-1860

6. E. Rolinski, G. Sharp, D.F. Cowgill and D.J. Peterman: J. Nuclear Mat. 252 (1998) 200-208
7. G. Lutjering: Materials Science and Engineering A263 (1999) 117-126
8. S.V. Gnedenkov, P.S. Gordienko, S.L. Sinebrukhov, O.A. Khrisanphova, and T.M. Skorobogatova: Corrosion, 56 (2000) 24-31
9. J.L. Murray and H.A. Wriedt: Bull. Alloy phase diagrams, 1987, 8, 148-165
10. Metals reference book: Colin J. Smithells ed., Batter worths & Co Ltd, London, UK (1976) 618
11. I.M. Poherlyuk: Materials Science 35(2) (1999) 284-289.
12. R. Hahn: J. Nucl. Mater., 245 (1997) 147
13. Y. Hatano, K. Isobe, R. Hitaka and M. Sugisake: J. Nucl. Sci. Technol., 33 (12) (1996) 944.

Table 1. Chemical composition of the Ti-Al-Zr alloy (wt.%)

Ti	Al	Zr	V	Fe	Co	S	C	O	N	H
95.24	2.25	2.24	0.06	0.05	0.14	0.0001	0.0090	0.0050	0.0004	0.0041

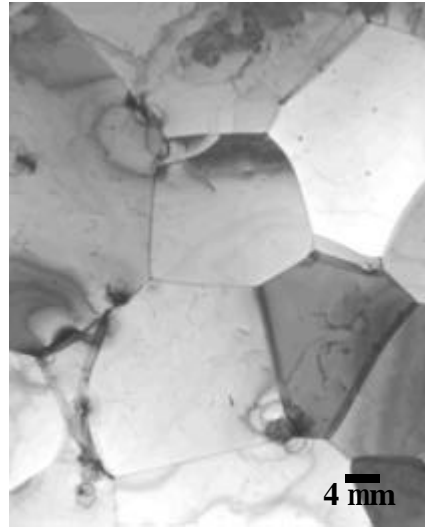


Fig. 1. Bright field TEM image of the longitudinal section of the as-received Ti-Al-Zr alloy tube.

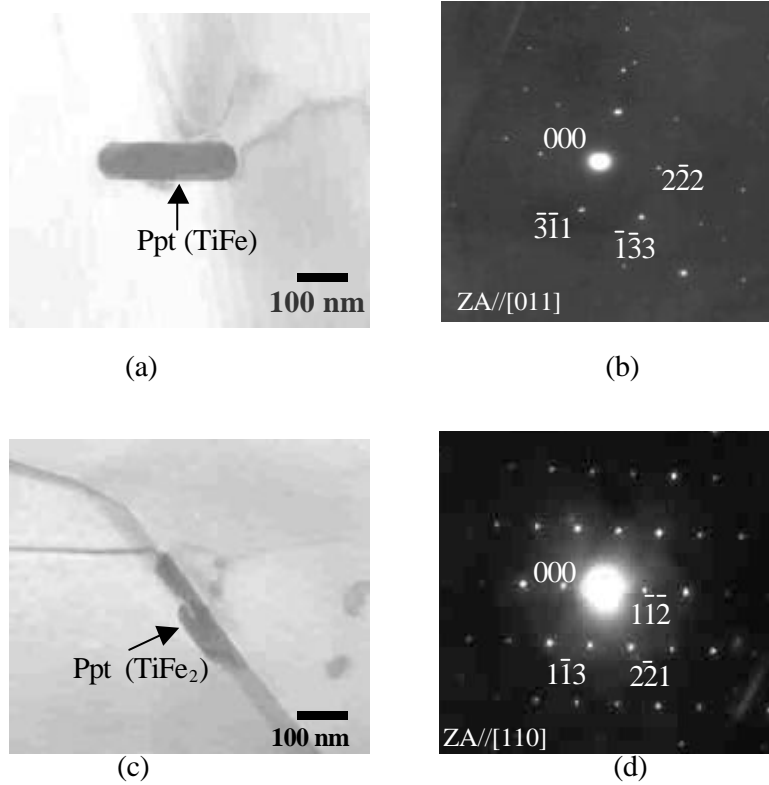
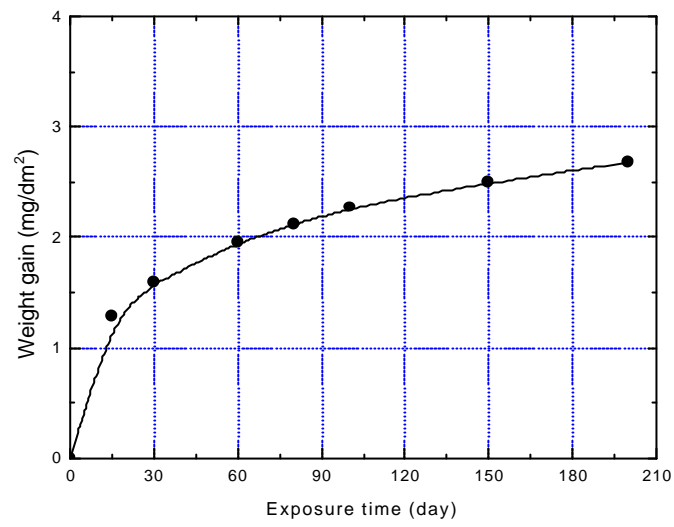
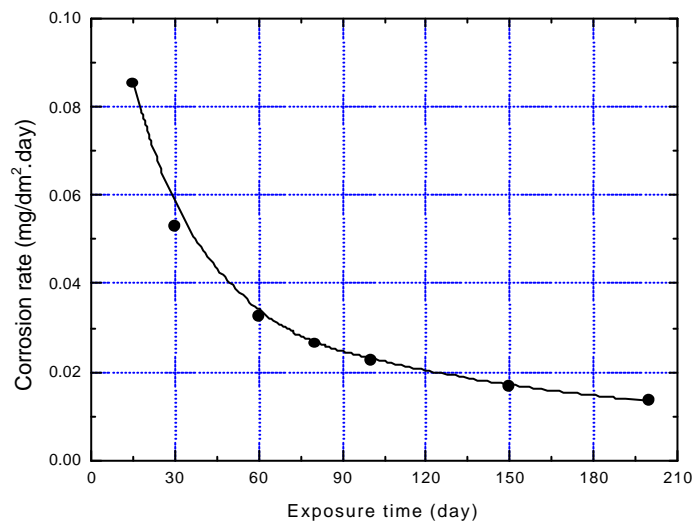


Fig. 2. Bright filed TEM images of precipitates in the Ti-Al-Zr alloy: (a) bright-field image (TiFe), (b) selected area diffraction pattern from precipitation allowed in (a), (c) bright-field image (TiFe₂), and (d) selected area diffraction pattern from precipitation allowed in (c).

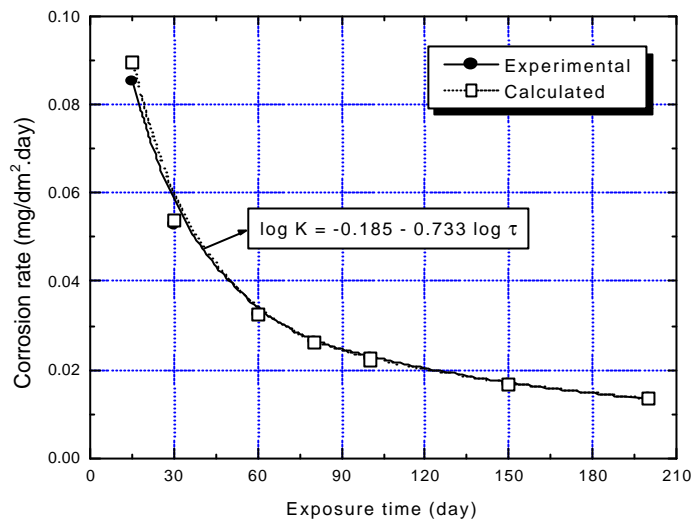


(a)

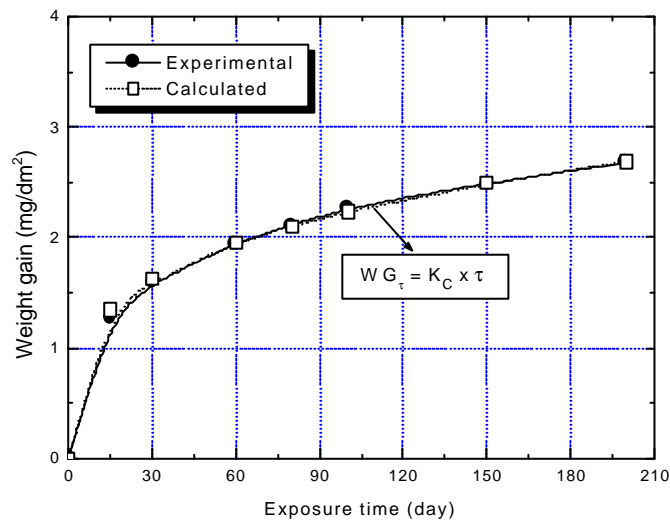


(b)

Fig. 3. Corrosion behavior of the Ti-Al-Zr alloy at 360 °C in a pH-9.98 ammonia aqueous solution: (a) weight gain, and (b) corrosion rate.



(a)



(b)

Fig. 4. Comparison of corrosion behavior obtained by experimental results with that calculated by the equation on the corrosion of the Ti-Al-Zr alloy: (a) corrosion rate, and (b) weight gain.

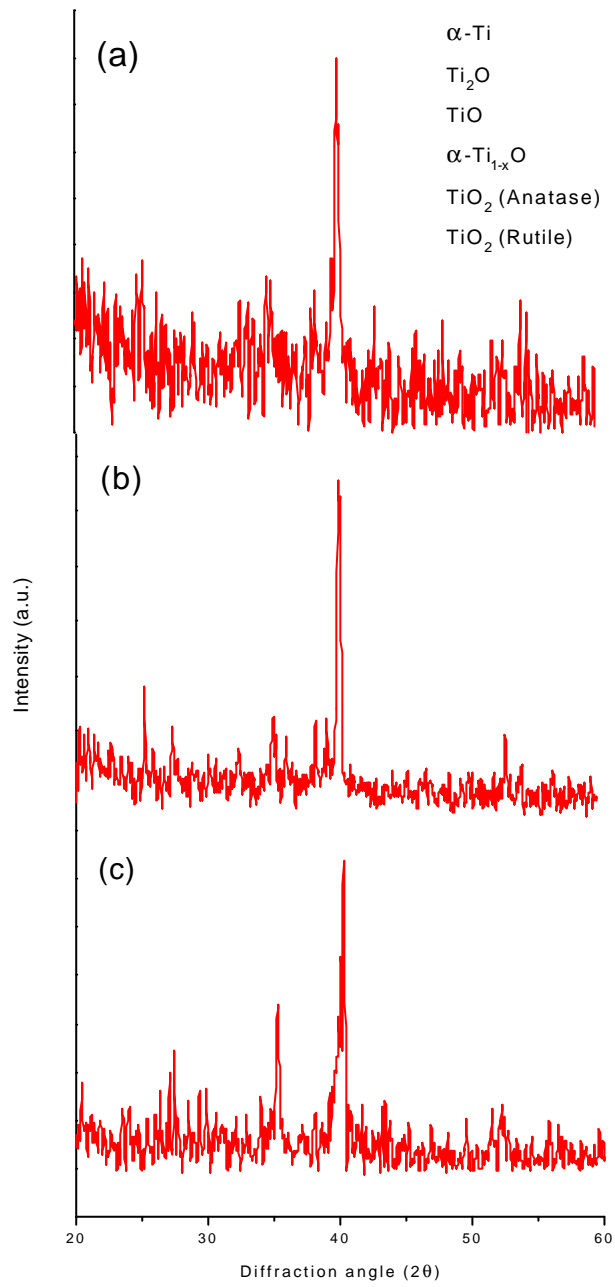


Fig. 5. X-ray diffraction patterns of the oxide scales formed in the surfaces of the Ti-Al-Zr alloy corroded at 360 °C for (a) 30, (b) 100 and (c) 200 days.

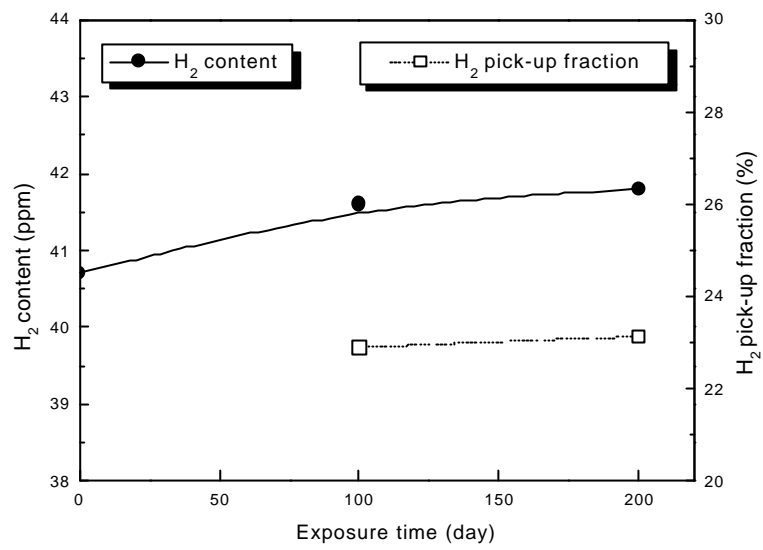


Fig. 6. Hydrogen contents and hydrogen pick-up fraction values of the Ti-Al-Zr alloy with exposure time.

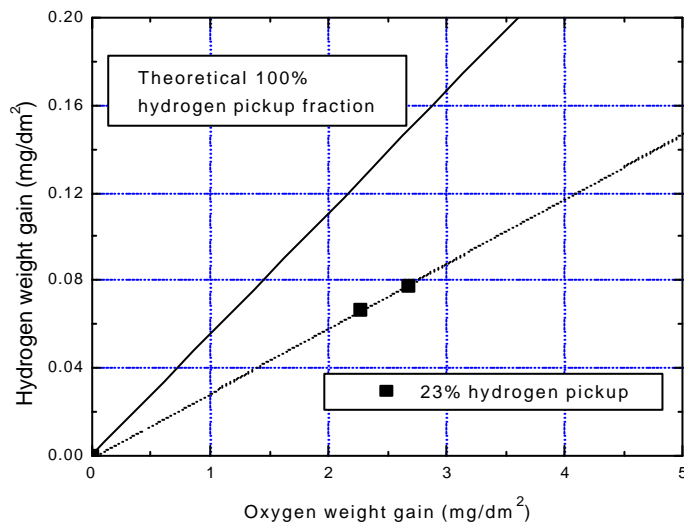


Fig. 7. Correlation of hydrogen pickup and oxygen weight gain in the corrosion of the Ti-Al-Zr alloy.

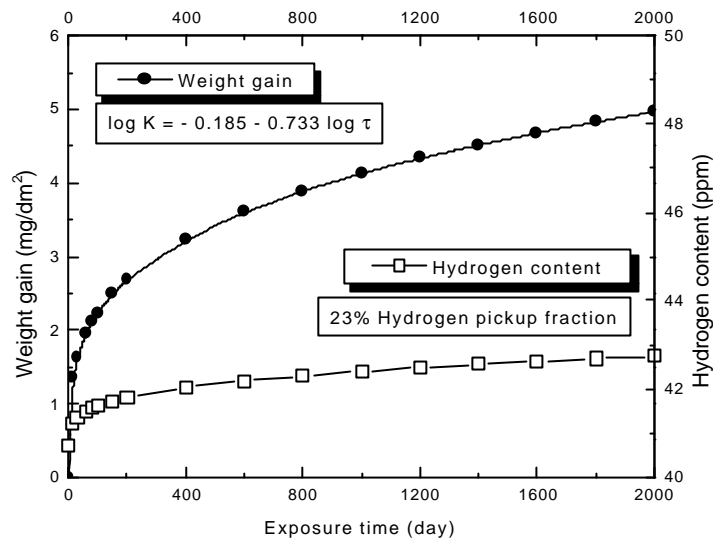


Fig. 8. Prediction of corrosion behavior and hydrogen content of the Ti-Al-Zr alloy during corrosion at 360 °C in a pH 9.98 alkaline solution for 2000 days, using a corrosion rate formula and hydrogen pickup fraction of 23%.

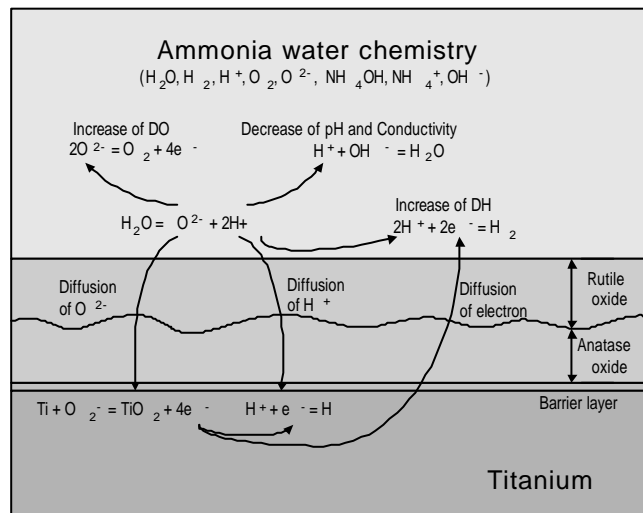


Fig. 9. Corrosion mechanism of the Ti-Al-Zr alloy at 360 °C in a pH 9.98 alkaline solution.